Self-assembly of regular hollow icosahedra in salt-free catanionic solutions

Monique Dubois*, Bruno Demé†, Thaddée Gulik-Krzywicki‡, Jean-Claude Dedieu‡, Claire Vautrin*, Sylvain Désert*, Emile Perez§ & Thomas Zemb*

** Service de Chimie Moléculaire (CEA/Saclay), F-91191 Gif sur Yvette Cedex, France*
† Institut Laue-Langevin, BP 156, F-38042 Grenoble Cedex 09, France
‡ Centre de Génétique Moléculaire, CNRS, F-91198 Gif sur Yvette, France
§ IMRCP, CNRS URA470, 118 route de Narbonne, F-31062 Toulouse, France

Self-assembled structures having a regular hollow icosahedral form (such as those observed for proteins of virus capsids) can occur as a result of biomineralization processes[1], but are extremely rare in mineral crystallites[2]. Compact icosahedra made from a boron oxide have been reported[3], but equivalent structures made of synthetic organic components such as surfactants have not hitherto been observed. It is, however, well known that lipids, as well as mixtures of anionic and cationic single chain surfactants, can readily form bilayers[4,5] that can adopt a variety of distinct geometric forms: they can fold into soft vesicles or random bilayers (the so-called sponge phase) or form ordered stacks of flat or undulating membranes[6]. Here we show that in salt-free mixtures of anionic and cationic surfactants, such bilayers can self-assemble into hollow aggregates with a regular icosahedral shape. These aggregates are stabilized by the presence of pores located at the vertices of the icosahedra. The resulting structures have a size of about one micrometre and mass of about 10^{10} daltons, making them larger than any known icosahedral protein assembly[7] or virus capsid[8]. We expect the combination of wall rigidity and holes at vertices of these icosahedral aggregates to be of practical value for controlled drug or DNA release.

Mixtures of anionic and cationic surfactants in water produce so-called 'catanionic' solutions. After ion pairing, counter-ions form excess salt and induce a high conductivity of the samples that screens electrostatic interactions. A particular type of salt-free catanionic formulation is obtained by using only H^+ and OH^- counter-ions, as no excess salt is then formed by mixing the two surfactants[9]. The resulting salt-free (also called true) catanionic systems can be represented in a ternary phase diagram whose two independent variables are the total volume fraction ϕ of surfactants (assuming surfactant density close to 1) and the molar fraction r of anionic surfactant over total surfactant content.

In dilute salt-free catanionic solutions, we have developed a simple method of producing self-assembled icosahedra of micrometre size in large quantities. Dilute solutions (below $\phi = 10^{-3}$) are prepared by adding water to appropriate amounts of the two surfactants, myristic acid ($M_W = 228.38$, Fluka, purity >99%) and cetyltrimethylammonium hydroxide (CTAOH) ($M_W = 301.54$, ethanolic solution from Acros Organics Co.). The monomer concentration of myristic acid is lower than 10^{-6} M, that is, quasi-insoluble in water. The critical micellar concentration, CMC, of CTAOH is slightly lower than CTABr which is 0.0013 mol l^{-1}. Rules for CMC of surfactant mixtures ensure that monomeric concentration is less than 10^{-6} M ($\Phi < 10^{-4}$)[10,11].

The solution is first heated to 60 °C for a few minutes, and then cooled to room temperature with permanent shaking during cooling, until transformation into a slightly bluish clear solution occurs. The solution does not contain any trace of insoluble material. The micrometre-sized icosahedra are formed upon cooling the salt-free catanionic solution, when the anionic component is in excess. Acceleration of the phase separation between a condensed lamellar phase and a fluid supernatant consisting of icosahedra can be induced by slight centrifugation at 3,000 *g*. Heating ensures re-dissolution and aggregates can be restored by cooling down again. Slow dissolution and gentle temperature cycles do not involve significant input of energy other than to disperse the small colloidal objects. Thus, the icoasahedral shape is only due to molecular interactions. As in the case of lipid microtubules[12], the aggregates are formed by cooling the sample through a first-order phase transition[13]. In our case, chain crystallization of ion pairs occurs while crossing the chain melting transition, determined by differential scanning calorimetry (DSC) to be in the range 50–65 °C depending on molar fraction r. Dilute solutions (less than 1 g l^{-1}) of icosahedra are metastable: mass measurements and freeze-fracture experiments can be done several weeks after preparation without noticeable change. Addition of glycerol prolongs the stability of the dispersion. However, after a period of the order of several months, a phase separation occurs: the top of the tube contains a thin layer of swollen lamellar phase (L_β).

The region where only icosahedra are formed is found in the range $0.5 < r < 0.75$ and for a total surfactant volume fraction $\phi < 10^{-3}$. The maximum volume fraction where micrometre-size aggregates are in a condition of close packing is $\phi = 3 \times 10^3$, as can be derived from simple geometrical evaluation. The structural electric charge of the aggregates is negative owing to the excess of myristic acid and rises with r up to 32 μC cm^{-2} for a known area per chain of 0.25 nm^2.

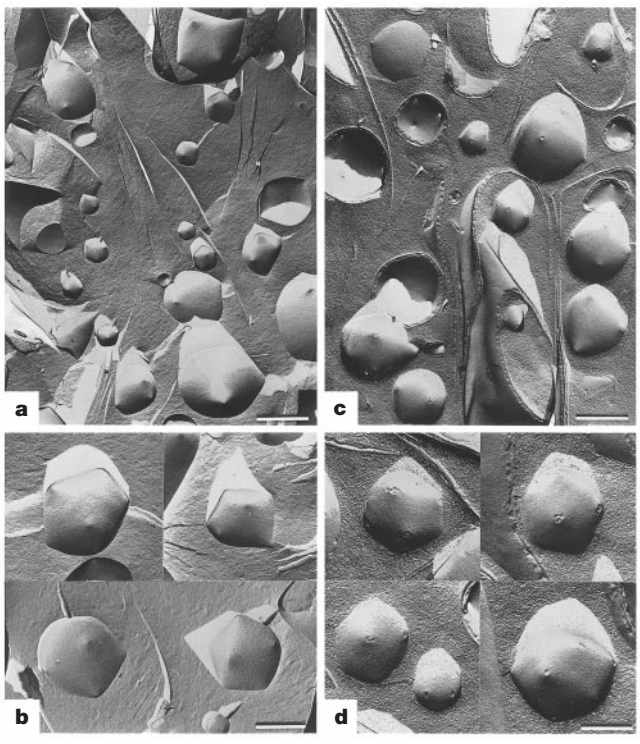

Figure 1 Electron microscopy images of icosahedral aggregates. Freeze fracture (**a**, **b**) and freeze-etching (**c**, **d**) obtained for a myristic acid–CTAOH sample ($r = 0.57$, initial weight fraction 0.0163 in a 1:2 glycerol/water solution). Samples were deposited on a thin copper holder, and rapidly quenched in liquid propane. Frozen samples were fractured in vacuum (10^{-7} torr) at –125 °C with a liquid-nitrogen-cooled knife in a Balzers 301 freeze-etching unit. The replication was done using unidirectional shadowing with platinum-carbon (35°, thickness 1–1.5 nm). **a**, **b**, The pores observable at vertices on freeze-fractured samples can be enlarged after the 5-min etching at –105 °C **c**, **d**, The scale bars represent 1 μm (**a**, **c**) and 500 nm (**b**, **d**).

Detection and characterization of dispersions containing icosahedra (Fig. 1) were primarily made by freeze-fracture and freeze-etching electron microscopy. Averaging over several hundreds of imaged objects, we find a narrow radius distribution in the range 700–1,000 nm, corresponding to an edge length of 1 μm. From simple geometrical considerations, and assuming that all objects are single-walled frozen bilayers, we evaluate that 2×10^7 catanionic pairs form one aggregate, which therefore has a molar mass close to 10^{10} Da. As can be seen in Fig. 2, the contour shape observed in freeze-fracture electron microscopy differs from symmetry apparent in cryo-TEM (transmission electron microscopy). At high magnification (Fig. 1b and d), a crucial feature appears: vertices of icosahedra consist of pores. The presence of holes and the associated electrostatic repulsions between them lead to regular polyhedra, which are different from closed-faceted vesicles[14] obtained, for instance, using a strongly adsorbed polymer[15].

For catanionic solutions in an excess of cationic component, nanodisks are formed by rejection of excess charges towards the edges[16]. The only other topology to evacuate excess charges is to segregate them in pores[17]. Vesicles present at high temperatures[5] with excess anionic component do not produce nanodisks upon cooling. The presence of excess insoluble fatty acid produces pores at vertices. These can be seen by electron microscopy or confocal microscopy. There are two ways of understanding the formation of pores by cooling vesicles: if the monolayer spontaneous curvature is close to zero while the gaussian curvature is negative, the presence of pores minimizes the bending energy[18,19]. Producing pores in the bilayer is a way for the system to self-assemble by minimising its curvature energy, since negative gaussian curvature is favoured at high surface charge[20,21]. Another mechanism at the origin of pore formation would be related to the absence of curvature singularity at vertices where a pore is present. The most frequent morphology of the aggregates is the icosahedron. However, we have observed the formation of other polyhedral shapes. These correspond to the family of structures with less than 12 vertices per polyhedra reviewed by Nelson and Spaepen[20]. Pores formed in these defect-stabilized structures are a privileged location for cationic solutes, impurities and probably oligopeptides (see Supplementary Information). As for catanionic nanodisks, in the absence of salt, molecular segregation is energetically possible owing to overwhelmingly strong electrostatic interactions[21].

Combined small-angle neutron and light scattering experiments (SANS and SALS, Fig. 3) provide independent proof that closed unilamellar objects of well-defined size are formed. The exact decay of the scattering as the second power of the scattering vector (q) and over an exceptionally wide range of vectors covered by light and neutron scattering at any concentration is evidence of the wall rigidity; the walls do not undulate under brownian motion. As for carbon nanotubes, the persistence length is in the micrometre range. Thus the elastic Young's modulus of the walls is of the order of at least 100 MPa, as for the nanodisks previously described[9]. The size and mass of the aggregates derived from these experiments coincide with those found by freeze-fracture electron microscopy. The minimum located at $q = 0.157\ \text{Å}^{-1}$ corresponds to the first minimum of the wall form factor oscillation and yields a bilayer thickness of 40 Å, close to the thickness of the nanodisks made of the same surfactant mixture.

In the dilute regime of salt-free catanionic mixtures, unilamellar vesicles form above the chain melting temperature[5]. During cooling down, the chain crystallization produces a two-dimensional array of alternated cationic and anionic heads. The array of crystallized chains has been characterized by wide-angle neutron scattering, using a mixture of perdeuterated anionic and protonated cationic components. Wide-angle neutron-scattering patterns obtained in the concentrated regime (L_β lamellar phase), suggest the presence of in-plane superstructures formed of alternated chains[22,23] $-CD_2-$ and $-CH_2-$ (see Supplementary Information). However, perfect order does not propagate over large distances, as is clear from the width of the in-plane superstructure peak and the absence of higher-order Bragg reflections. The excess of anionic surfactant is segregated during crystallization of the faces. The amount of excess anionic component is such that 12 pores per vesicle are formed (see the confocal microscopy images indicating the specific location of the charged dye in the Supplementary Information).

Pores formed during crystallization are charged and repel due to the absence of screening salt (Debye screening length of the order of

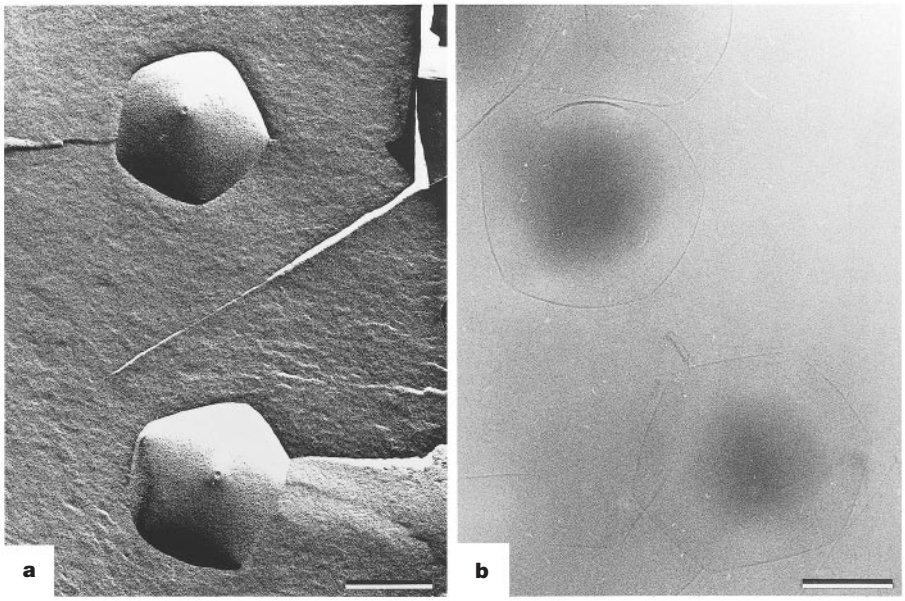

Figure 2 Comparison of freeze-fracture (**a**) and cryo-TEM (**b**) images for two adjacent aggregates. We note the systematic presence of five vertices as first neighbours centred on a given vertex. Freeze-fracture suggests pentagonal symmetry around a vertex, whereas the TEM images enhance bilayers normal to the image showing the hexagonal shape, which is expected for an equatorial fracture through an icosahedron. The icosahedron is the only structure which appears to be hexagonal on projection and pentagonal after fracture. The scale bars represent 250 nm.

100 nm). The structure that minimizes the bending energy with the electrostatic constraints is a regular icosahedron. Any other regular polyhedra would increase the free energy of the aggregate.

Formation of icosahedra with a preferred diameter of 2 μm is controlled both by thermodynamics and kinetics. At high temperature, thermodynamically stable vesicles are present above the chain-melting temperature. During crystallization, bilayers expel laterally a small part of the component in excess, which is not miscible in the two-dimensional crystal. This step is kinetically controlled and leads to the formation of a certain density of pores. If the density of pores is too low or too high, icosahedra cannot form and planar fragments are found (see phase diagram and micrographs in the Supplementary Information).

The method described here is an example of a general principle of formation of icosahedra using given number of surfactant pairs with appropriate chain length and headgroup volumes. The three conditions for formation of regular icosahedra are:

(1) A domain of compositions in the phase diagram where vesicles are the stable form at high temperature. The corresponding region at room temperature is a tie line between a swollen lamellar phase with frozen chains and water.

(2) The excess of surfactant must be insoluble in water and in the frozen bilayer forming the planar rigid walls. This excess surfactant easily forms pores on its own owing to the packing properties of unscreened charged surfactant headgroups[21].

(3) The part of excess component segregated by the two-dimensional crystal of frozen chains must be available in a sufficient quantity to form twelve pores per vesicle.

These rules apply for all surfactant pairs studied so far. The absence of condition (3) leads to the formation of nanodisks or large opened crystalline bilayers including pores (see Supplementary Information). Negatively charged icosahedra of identical size are formed in pure water or in water/glycerol mixtures (2:1 by weight).

Typical conductivity of solutions containing icosahedra ($r \approx 0.65$) is 10 μS cm^{-1} for an apparent pH of 5.6 measured with a calomel electrode. Strong electrostatic repulsions between icosahedra explain the observed kinetic stability. After a few months at rest, a thin layer of lamellar phase appears at the top of the test tube. The high rigidity of the faces quenches the so-called 'Helfrich' repulsive interaction, when an icosahedron comes into contact with a rigid interface, by at least a factor of hundred. These are very different from soft single-layer or multilayer vesicle[24] structures widely used for drug delivery or penetration of creams through the skin in cosmetic applications. Holes at vertices can be covered by an adequate polyelectrolyte, as already described for the preparation of microcapsules[23]. This property would be important for controlled drug or DNA release, if the aggregates described here were resistant to the addition of even small quantities of salt. However, phase separation between a lamellar phase (L_β) and nearly pure water is observed at high ionic strength. In the presence of small quantities (millimoles) of salt or impurities, or after incubation in pure water, we have observed, using confocal microscopy, large flocculates made of several icosahedra adhering to each other much as do a bunch of grapes. These globular aggregates, whose typical size is five to ten micrometres, visible in optical microscopy, are built with irregular polyhedra with flat faces. Their morphology is different from the well known myelinic figures, but they show a topology very similar to biliquid foams made from multivesicular liposomes which have been described by Spector *et al.*[24].

Thus we have demonstrated that single-wall icosahedra are formed by cooling solutions of vesicles of appropriate composition

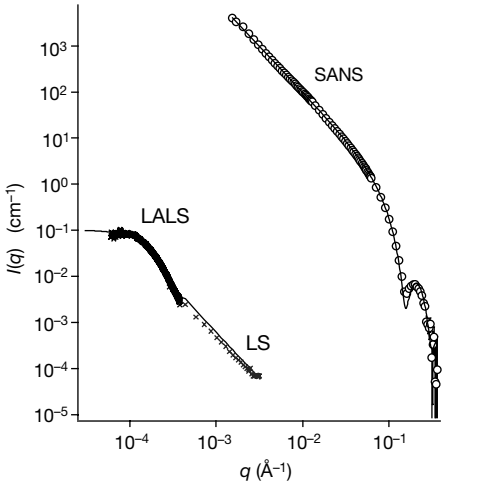

Figure 3 Scattering by dilute solutions of icosahedra. We used small-angle neutron scattering (SANS), low-angle light scattering (LALS) and classical light scattering (LS) covering a q-range: $5 \times 10^{-5} < q < 4 \times 10^{-1}$ Å^{-1}. Neutron scattering composition of the sample: $r = 0.636$, $\phi = 2.6 \times 10^{-3}$. Light scattering $r = 0.626$, $\phi = 1.3 \times 10^{-4}$ in glycerol/water. The SANS instrument used D22 (ILL, Grenoble). LS results are compared to a simulation of the scattering produced by independent icosehedra (form factor calculated for a gaussian distribution with average radius of 0.9 μm, and full-width at half-maximum, FWHM = 0.6 μm). SANS shows an ideal q^{-2} dependence over four decades in intensity, followed by the characteristic oscillation of the shell form factor with the first minima at $q = 0.157$ Å^{-1} corresponding to the membrane thickness. The solid line is a fit to the data using a three-layer model for infinitely flat membranes convoluted by the instrumental resolution function accounting for the wavelength spread and finite spatial resolution of the camera. It yields a bilayer thickness $2t = 40$ Å. The average mass M of the icosahedra is extracted from the LALS data at zero angle, yielding 2×10^{10} Da/icosahedron. ($M = 8.66\rho l^2 2t$, where l is the edge length, and ρ the density close to 1).

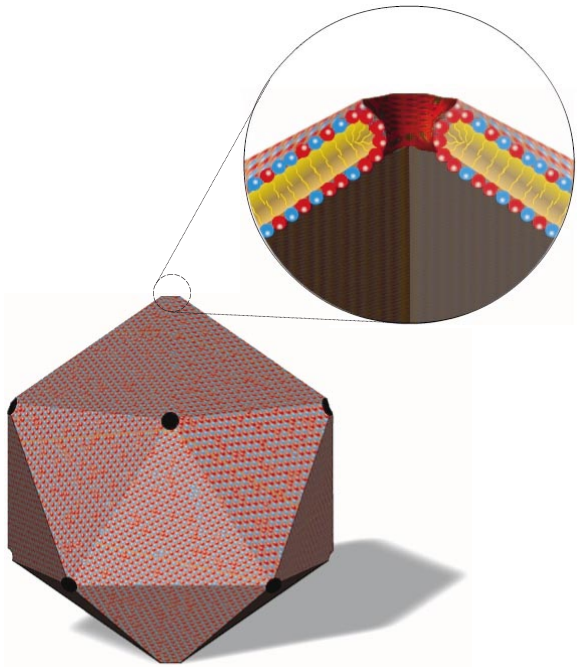

Figure 4 Sketch of the aggregate structure. Frozen alternated hydrocarbon chains produce large flat faces made of about 10^6 ion pairs. These triangular faces, with a typical area of 0.3 μm^2, result from the juxtaposition of ion pairs tiling an hexagonal lattice. The aggregates are stabilized by the pores (diameter of the order of 150 Å) produced by about 200 molecules and due to the partial segregation of the anionic surfactant in excess. The regular icosahedron is the structure that minimizes the bending energy of rigid bilayers, as only 30 edges with a dihedral angle of 42° delimit triangular faces.

and in the absence of salt using only two synthetic surfactants. The microstructure of these complex aggregates is sketched in Fig. 4. Self-assembly of icosahedra, owing to defect-free repetition of strong interactions, is one of the fascinating consequences of the quasi-equivalence principle[25]: highly symmetric structures can be formed with high efficiency by association of identical subunits in the absence of templates. The self-assembled two-dimensional nearly crystalline shell is similar in shape to the structure initially proposed for viruses by Watson and Crick[26]. In catanionic icosahedra, subunits are combinations of catanionic pairs. Although in viruses the number of subunits is smaller, the type of aggregates described here should obey a similar topology control mechanism: a locally hexagonal lattice folds into 20 equivalent triangles. The association of anionic and cationic surfactants produces particles similar in shape but larger than viruses. □

Received 14 February; accepted 27 March 2001.

1. Thompson, D. W. *On Growth and Form* (Cambridge Univ. Pres, Cambridge, 1961).
2. Kimoto, K. & Nishida, I. The crystal habits of small particles of aluminium and silver prepared by evaporation in clean atmosphere of argon. *J. Appl. Phys.* **16,** 941–948 (1966).
3. Hubert, H. H. *et al.* Icosahedral packing of B_{12} icosahedra in boron suboxide. *Nature* **391,** 376–378 (1998).
4. Sackmann, E. & Lipowsky, R. *Handbook of Biological Physics* Vol. 1B (ed. Hoff, A. J.) (North-Holland, Amsterdam, 1995).
5. Kaler, E. W., Murthy, A. K., Rodriguez, B. E. & Zasadzinski, J. A. N. Spontaneous vesicle formation in aqueous mixtures of single-tailed surfactants. *Science* **245,** 1371–1374 (1989).
6. Dubois, M. & Zemb, T. Swelling limits for bilayer microstructures: the implosion of lamellar structure versus disordered lamellae. *Curr. Opin. Colloid Interf. Sci.* **5,** 27–37 (1997).
7. Wals, J. *et al.* Tricord protease exists as an icosahedral supermolecule *in vivo*. *Molecul. Cell.* **1,** 59–65 (1997).
8. Klug, A., Franklin, R. E. & Humphrey-Owen, S. P. F. The crystal structure of Tipula iridescent virus as determined by Bragg reflection of visible light. *Biochem. Biophys. Acta* **32,** 203–219 (1959).
9. Dubois, M., Gulik-Kryzwicki, Th., Demé, B. & Zemb, T. Rigid organic nanodiscs of controlled size: A catanionic formulation. *C. R. Acad. Sci. Paris II C* **1(9),** 567–575 (1998).
10. Scamehorn, J. F. & Hartwell, J H. in *Surfactant Science Series* (eds Scamehorn, J. F. & Harwell, J. H.) Vol. 33, Ch. 10 (Marcel Dekker Inc., New York, 1989).
11. Graciaa, A., Ghoulam, M. B., Marion, G. & Lachaise, J. Critical concentrations and compositions of mixed micelles of sodium dodecylbenzesulfonate, tetradecyltrimethylammonium bromide and polyethylenephenols. *J. Phys. Chem.* **93,** 4167–4173 (1989).
12. Schnur, J. Lipid tubules: a paradigm for molecularly engineered structures. *Science* **262,** 1669–1675 (1993).
13. Thomas, B. N., Safinya, C. R., Plano, R. J. & Clark, N. A. Lipid tubules self-assembly: length dependence on cooling rate through a first-order phase transition. *Science* **227,** 1635–1638 (1995).
14. Parente, R. A., Höchli, M. & Lentz, B. R. Morphology and phase behavior of two types of unilamellar vesicles prepared from synthetic phosphatidylcholines studies by freeze-fracture electron microscopy and calorimetry. *Biochim. Biophys. Acta* **812,** 493–502 (1985).
15. Regev, O., Marques, E. F. & Khan, A. Polymer-induced structural effects on catanionic vesicles: formation of faceted vesicles, disks, and cross-links. *Langmuir* **15,** 642–645 (1999).
16. Zemb, T., Dubois, M., Demé, B., Gulik-Krzywicki, T. Self-assembly of flat nanodiscs in salt-free catanionic surfactant solutions. *Science* **283,** 816–820 (1999).
17. Hyde, S. T. Topological transformations mediated by bilayer punctures: from sponge phases to bicontinuous monolayers and reversed sponges. *Colloids Surf. A* **129–130,** 207–225 (1997).
18. Fogden, A., Daicic, J. & Kidane, A. Undulating charges in fluid membranes and their bending constants. *J. Phys. (Paris) II* **7,** 229–248 (1997).
19. Fogden, A. & Daicic, J. & Kidane, A. Bending rigidity of ionic surfactant interfaces with variable charge density: the salt-free case. *Colloids Surf. A* **129–130,** 157–165 (1997).
20. Nelson, D. R. & Spaepen, F. Polytetrahedral order in condensed matter. *Solid State Phys.* **42,** 1–90 (1989).
21. Dubois, M., Belloni, L., Zemb, T., Demé, B. & Gulik-Krzywicki, T. Formation of rigid nanodiscs: Edge formation and molecular separation. *Prog. Colloid Polym. Sci.* **115,** 238–242 (2000).
22. Radtchenko, I. L. *et al.* Assembly of alternated mutlivalent ion/polyelectrolyte layers on colloidal particles. Stability of the multilayers and encapsulation of macromolecules into polyelectrolyte capsules. *J. Colloid Interf. Sci.* **230,** 272–280 (2000).
23. Donath, E., Sukhorukov, G. B., Caruso, F., Davis, S. A. & Möhwald, H. Novel hollow polymer shells by colloid-templated assembly of polyelectrolytes. *Angew. Chem. Int. Edn* **37,** 2202–2205 (1998).
24. Spector, M. S. & Zasadsinski, J. A. Topology of multivesicular liposomes, a model biliquid foam. *Langmuir* **12,** 4704–4708 (1996).
25. Klug, A. & Caspar, D. L. D. The structure of small viruses. *Adv. Vir. Res.* **7,** 225–325 (1960).
26. Crick, F. H. & Watson, J. D. The structure of small viruses. *Nature* **177,** 473–475 (1956).

Supplementary information is available from *Nature*'s World-Wide Web site (http://www.nature.com) or as paper copy from the London editorial office of *Nature*.

Acknowledgements

We thank G. Sukhorukov and O. Tiourina for help in confocal optical microscopy, and I. Erk for cryo-TEM. We also thank J.-L. Sikorav, P. Timmins and B. W. Ninham for critical reading of the manuscript and suggestions.

Correspondence and requests for materials should be addressed to M.D. (e-mail: duboism@scm.saclay.cea.fr).

Stability of atmospheric CO_2 levels across the Triassic/Jurassic boundary

Lawrence H. Tanner*, John F. Hubert†, Brian P. Coffey‡§ & Dennis P. McInerney‖

* *Department of Geography and Geosciences, Bloomsburg University, Bloomsburg, Pennsylvania 17815, USA*
† *Department of Geosciences, University of Massachusetts, Amherst, Massachusetts 01003, USA*
‡ *Department of Geological Sciences, Virginia Polytechnic Institute and State University, Blacksburg, Virginia 24061, USA*
‖ *Environmental Risk Management, Fleet National Bank of Connecticut, Hartford, Connecticut 06102, USA*

The Triassic/Jurassic boundary, 208 million years ago, is associated with widespread extinctions in both the marine and terrestrial biota. The cause of these extinctions has been widely attributed to the eruption of flood basalts of the Central Atlantic Magmatic Province[1–4]. This volcanic event is thought to have released significant amounts of CO_2 into the atmosphere, which could have led to catastrophic greenhouse warming[5–7], but the evidence for CO_2-induced extinction remains equivocal. Here we present the carbon isotope compositions of pedogenic calcite from palaeosol formations, spanning a 20-Myr period across the Triassic/Jurassic boundary. Using a standard diffusion model[8,9], we interpret these isotopic data to represent a rise in atmospheric CO_2 concentrations of about 250 p.p.m. across the boundary, as compared with previous estimates of a 2,000–4,000 p.p.m. increase[4,5]. The relative stability of atmospheric CO_2 across this boundary suggests that environmental degradation and extinctions during the Early Jurassic were not caused by volcanic outgassing of CO_2. Other volcanic effects—such as the release of atmospheric aerosols or tectonically driven sea-level change—may have been responsible for this event.

The mass extinction at the end of the Triassic claimed about 80% of all species[10], including most non-dinosaurian archosaurs[11]. Although extinctions in the terrestrial and marine environments may be slightly asynchronous, they are closely related temporally and undoubtedly share causality[12]. This biotic crisis has been attributed previously to bolide impact[6,13] and sea-level change[14,15]. However, dating of the best-candidate impact structure (the Manicouagan crater) places the impact roughly 14 Myr earlier[16], and sea-level change fails to explain the fern spike in the terrestrial boundary record[6]. The prevailing view is that this event resulted from the eruptions of the Central Atlantic Magmatic Province (CAMP), which may have produced as much as 7×10^6 km^2 of flood basalt in as little as 2 Myr[3]. CAMP volcanics include the basalts of the Newark Supergroup of eastern North America whose ages of around 200 Myr and stratigraphical proximity to the Triassic/Jurassic boundary are well constrained[12,17]. A frequently cited deleterious effect of these widespread, massive eruptions is a sudden increase in

§ Present address: ExxonMobil Upstream Research Company, Houston 77252, Texas, USA.